OPTIMIZATION OF INKJET NOZZLE PARAMETERS BY COMPUTATIONAL ANALYSIS FOR INKJET APPLICATIONS

ME8811 - PROJECT WORK

Submitted by

AKSHAY KUMAR G V

DHAYAHAR G D

PALANI KARTHICK S

KARAN S

In partial fulfilment for the award of the degree

of

BACHELOR OF ENGINEERING

in

MECHANICAL ENGINEERING

PSG INSTITUTE OF TECHNOLOGY AND APPLIED RESEARCH,
NEELAMBUR -641062

ANNA UNIVERSITY: CHENNAI 600025

AUGUST 2021

ACKNOWLEDGEMENT

We wish to express my sincere thanks to Dr. G. CHANDRAMOHAN, Principal, PSG Institute of Technology and Applied Research for his support in carrying out the project as a part of our curriculum.

We express our gratitude to Dr. N. SARAVANAKUMAR, Head of the Department, Department of Mechanical Engineering, PSG Institute of Technology & Applied Research for his constant encouragement throughout the project work.

We express our gratitude to Dr. P. MANOJ KUMAR, Associate Professor, Department of Mechanical Engineering who gave valuable guidance in helping to complete the project. Thank you for your comments on the methodologies and suggestions.

ANNA UNIVERSITY: CHENNAI 600 025

BONAFIDE CERTIFICATE

Certified that this project report titled **"OPTIMIZATION OF INKJET NOZZLE PARAMETERS BY COMPUTATIONAL ANALYSIS FOR INKJET APPLICATIONS"** is the bonafide work of **AKSHAYKUMAR G V**, **DHAYAHAR G D, PALANI KARTHICK S, KARAN S** who carried out the project work under my supervision.

SIGNATURE **HEAD OF THE DEPARTMENT** **(Dr. N. SARAVANAKUMAR)**	**SIGNATURE** **SUPERVISOR** **(Dr. P. MANOJ KUMAR)**
Head of the Department, Department of Mechanical Engineering, PSG Institute of Technology and Applied Research, Coimbatore	Associate Professor, Department of Mechanical Engineering, PSG Institute of Technology and Applied Research, Coimbatore

Submitted for the university examination held on ____________________.

INTERNAL EXAMINER

EXTERNAL EXAMINER

ABSTRACT

Today, there are many technologies that have been developed in field of inkjet nozzle right from design to manufacturing of nozzle. But however, one of the main things for usage of inkjet nozzle is analysis and optimization of nozzle for specified application. There are few methods available for analysis and optimization of inkjet nozzle. At present inkjet nozzle is used in wide variety of application starting from small transistors and MEMs to large pharmaceutical applications. Here, in this work an attempt is made to analyze and optimize the nozzle and also to examine its scope for improvement.

TABLE OF CONTENTS

LIST OF TABLES

LIST OF FIGURES

CHAPTER 1

INTRODUCTION

Nowadays, there has been many investments in development for inkjet nozzle in recent years. This is because of versatility of inkjet nozzle in several areas. Inkjet nozzle uses are at high standards in present time. And also ease of manufacturing technique at present makes inkjet technology to use in a wider space application. With other advantages like easier operation, finer printing compared to other methods like dye sublimation and laser printing, very high-speed printing. Some of the applications include Thin film transistor, light emitting devices, memory and magnetic applications, contacts and conducting devices, sensors and detectors, biological and pharmaceutical application, fuel cell, solar cells, textiles, ceramics, 3D printing etc.

1.1 INKJET PRINTING

Inkjet printing is a material-conserving deposition technique used for liquid phase materials. These materials, or inks, consist of a solute dissolved or otherwise dispersed in a solvent. The process involves the ejection of a fixed quantity of ink in a chamber, from a nozzle through a sudden, quasi-adiabatic reduction of the chamber volume via piezoelectric action. A chamber filled with liquid is contracted in response to application of an external voltage. This sudden reduction sets up a shockwave in the liquid, which causes a liquid drop to eject from the nozzle. This process has been analyzed at some length and the reader is referred to recent review papers. The ejected drop falls under action of gravity and air resistance until it impinges on the substrate, spreads under momentum acquired in the motion, and surface tension aided flow along the surface. The drop then dries through solvent evaporation. Recent studies show that drop spreading and the final printed shape strongly depend on the viscosity, which in turn is a function of the molar mass of the polymer. More interestingly, the aforementioned group also found a printing height dependence of the final dried-drop diameter, which was a function of the polymer concentration. There are two basic type of inkjet printing. namely

- Continuous inkjet method
- Drop on demand method

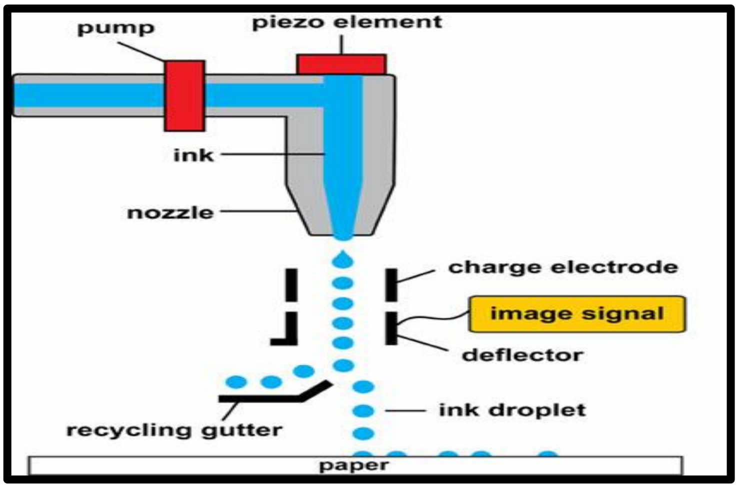

Figure 1.1 Continuous Inkjet

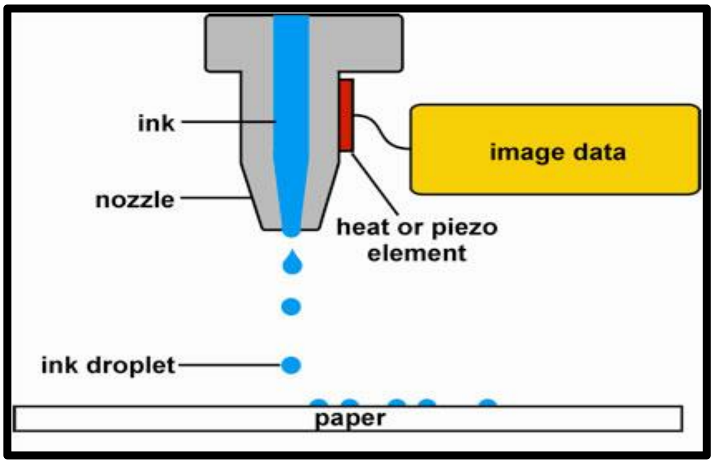

Figure 1.2 Drop On Demand Inkjet

1.1.1 CONTINUOUS INKJET METHOD

The simplest way of generating droplets of controlled size and velocity is with continuous inkjet printing. A pressure pump causes a continuous jet of ink from the nozzle. The eventual droplet size is controlled with a piezoelectric actuator. After leaving the nozzle, the droplets are selected to be printed or to be recycled. The unnecessary droplets are charged by an electrode close to the nozzle and directed toward a recycling gutter by an electric field.

At low jet velocity, it is easy to make such a strong velocity perturbation that the jet breaks up into droplets purely by the velocity fluctuation at the nozzle. When the jet velocity is increased, the relative fluctuation caused by the piezo decreases, and the jet breakup occurs not at the nozzle but further downstream.

These printers are large and have only been used in commercial printing environments. The use of these devices for printing individual images has dramatically declined, but the technology is currently being repurposed into some other applications. Continuous inkjet printing is mainly used for coding in the packaging industry, due to its high speed and reliability.

1.1.2 DROP ON DEMAND METHOD

Since its invention in the second half of the twentieth century, DOD inkjet printing has been applied mainly for graphics printing. Recently, it has also been used in additive manufacturing, textile printing, home decorations, and many more applications. This broad variation of applications demands a broad range of inks and print heads. The droplet can vary between 200 fl for high-detail functional printing and 200 nl for high-speed decorative patterning applications. The drop size and velocity can be varied by using different nozzle sizes but also by using different driving strategies. In Figure given below, the drop formation cycles for two different actuation amplitudes are shown. At a low amplitude, the ligament pinches off at the nozzle.

The tail droplet that forms due to the capillary contraction of the ligament has sufficient velocity to catch up with the slow head droplet. When the amplitude is high, the head droplet has such a high velocity that the tail droplet cannot reach the head droplet before the tail breaks up into the Rayleigh–Plateau instability. For some applications, such as the printing of random patterns on ceramic floor tiles, the presence of these satellite droplets is not an issue. For functional printing, where, for example, conductive wires are printed, the satellite droplets are unacceptable. Printing accuracy and productivity increase with drop velocity, but the generation of satellite droplets also increases with drop velocity. It is a challenge in DOD inkjet printing research to find nozzle geometries and actuation signals that result in fast drops without satellite droplets.

Here, we show two sequences of photographs taken from a drop-on demand drop formation cycle. The droplets are recorded by single flash stroboscopic. In the left sequence, the actuation signal has a low amplitude, resulting in a slow droplet. The tail remains stable until the tail droplet is merged with the head droplet due to capillary contraction of the ligament. In the sequence on the right, the actuation signal amplitude is 25% higher. The droplet is so fast that the tail droplet cannot merge with the head droplet before the tail has broken up. Eventually, the tail droplet merges with the head droplet.

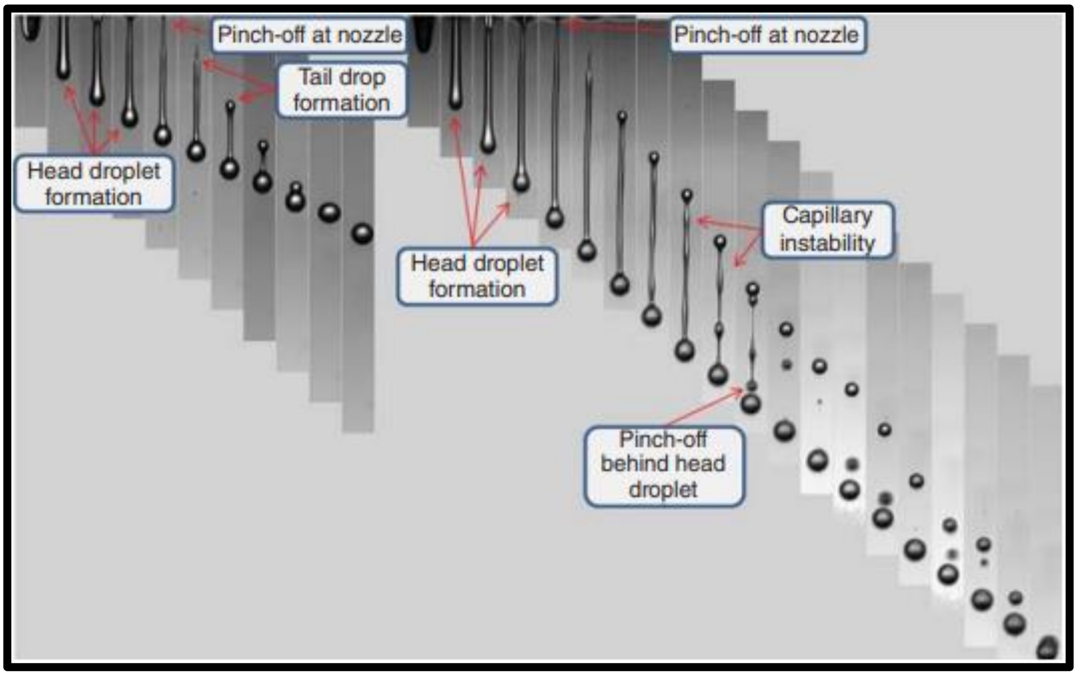

Figure 1.3 Drop Formation

1.2 DROP FORMATION IN CONTINUOUS INKJET AND DROP-ON-DEMAND

In both the CIJ and DOD methods, the liquid ink flows through a small hole (usually called a nozzle). The essential difference between the two methods lies in the nature of the flow through the nozzle. In CIJ, as the name implies, the flow is continuous, while in DOD, it is impulsive.

A CIJ system produces a continuous stream of drops, from which those to be printed on to the substrate are selected as required, whereas in DOD printing, the ink is emitted through the nozzle to form a short jet, which then condenses into a drop, only when that drop is needed. A continuous stream of liquid merging from a nozzle is inherently unstable and will eventually break up into a stream of droplets under the influence of surface tension forces.

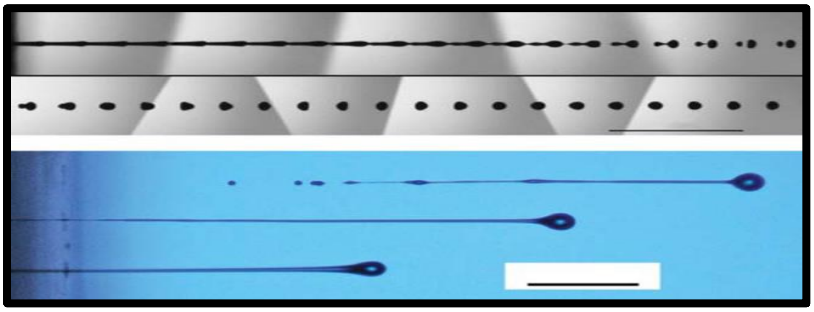

Figure 1.4 Droplet formation in CIJ and DOD

1.2.1 PIEZOELECTRIC DROP GENERATION

In piezo DOD, a voltage-driven piezoelectric transducer is used to mechanically deform the walls of the ejection chamber to eject a droplet. Each nozzle is driven by a separate transducer, and when a voltage is applied, it produces an electric field across a layer of piezoelectric material that causes the transducer to deform. The deformation causes the volume of the ejection chamber to contract or expand depending on the polarity of the applied voltage. This controls the pressure within the chamber, that is, higher pressure when the chamber contracts and lower pressure when it expands. A custom voltage waveform is applied to provide a desired time-dependent pressure within the chamber to optimize both droplet ejection and refill of the chamber.

The simulation of piezo DOD involves both FSI (Fluid-Structure Interaction), that is, the coupled motion of the transducer and the fluid, and FSA (Free Surface Analysis) to track the surface of the ink throughout the ejection cycle. Specifically, FSA is needed to track the motion of the ink meniscus in the nozzle during the initial stages of ejection, the surface of the ejected mass of ink as it evolves into a droplet, and the meniscus of the ink in the ejection chamber during refill.

A major challenge in simulating piezoelectric DOD involves the accurate prediction of FSI, that is, two-way coupling between the transducer as it deforms and the resulting change in the flow field within the ink. As the transducer deforms, it displaces ink, and the flowing ink provides a pressure load on the transducer that impacts its deformation.

A rigorous analysis of this process requires the simultaneous and self-consistent calculation of both the ink and structural dynamics. However, the majority of piezo DOD models do not take into account fully coupled FSI (Fluid – Structure Interface). Instead, the ejection process is often simplified, either by assuming a limited one-way coupling wherein the transducer deformation ejects ink but the back reaction of the ink on the transducer is ignored or by ignoring mechanical actuation altogether and replacing it with a time-dependent pressure condition in the ejection chamber.

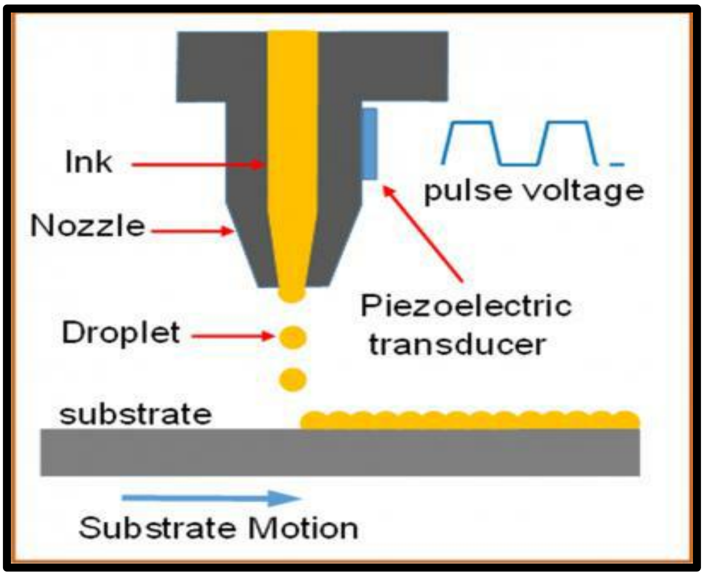

Figure 1.5 Piezoelectric Drop Formation

1.2.2 THERMAL DROP GENERATION

A thin-film resistive heater is integrated into a wall of the ejection chamber. When a droplet is desired, the heater is activated using a short (microsecond)-duration voltage pulse. The voltage is of sufficient magnitude to raise the temperature of a thin layer of ink in contact with the wall (above the heater) to its superheat temperature, approximately 300°C for water under atmospheric pressure.

Once the superheat temperature is reached, the ink evaporates explosively and forms a homogeneous vapour bubble, with a high initial pressure (>100 bar). Given this pressure, the bubble expands rapidly within the ink chamber and ejects ink through the nozzle with enough momentum to form a droplet with a desired volume. The bubble subsequently collapses and the chamber refills with ink from a reservoir due to capillary pressure provided by surface tension.

A rigorous analysis of TIJ droplet ejection is complicated. It includes the prediction of voltage-driven excitation of a resistive heater, heat transfer from the heater to the ink, phase change from superheated ink to vapour, vapour bubble dynamics, drop ejection, refill of the ejection chamber, and the formation (pinch-off) of the ejected droplet. In some models, the analysis is simplified by imposing a time-dependent pressure BC (Boundary Conditions) that mimics the pressure exerted by the bubble as it expands. Given an imposed pressure, a CFD/FSA is used to predict the mass of ink ejected through the nozzle and subsequent droplet formation.

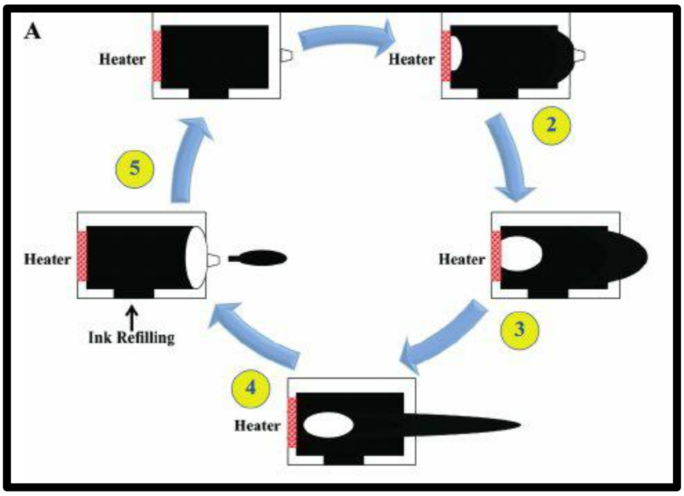

Figure 1.6 Thermal Drop Generation

1.3 APPLICATIONS

Inkjet printing has wide range of applications. Some of them are as follows

- Initially this method was found only to print images on paper but later when found its true potential found applications in other areas as well some of these include areas where high precision materials deposition is required like material deposition for OLED and solar cells.
- In some countries it is also in machinery and currency for printing Barcode because of its print quality and precision.
- It is also used in biomedical applications for drug discovery and for synthesis of cells and tissues.
- It is used for printing carbon supported platinum 3D layers which is used as catalyst in fuel cell as it causes less wastage at the edges.
- It is also used in 3D printing of ceramic materials.

CHAPTER 2

LITERATURE SURVEY

2.1 STUDIES AND WORK PERFORMED BY VARIOUS PEOPLE IN THEIR JOURNALS

Fuel cells are rapidly gaining attention as alternatives to current power sources due to their high efficiencies and ability to operate without greenhouse gas emissions. One of the obstacles preventing the commercialization of fuel cells is the utilization of noble metals, most often platinum or platinum-based alloys, to catalyze the oxidation and reduction reactions. Methods for producing Pt nanoparticles supported on carbon have helped to lower platinum loadings in PEMFCs. Although research reduced catalyst loading levels down from 4 to below 0.4 mg Pt cm^{-2}, the Pt utilization of typical commercially offered prototype fuel cells remains very low (20–30 %). Thin film deposition such as sputtering have been investigated for catalyst deposition at ultra-low loadings. While this method could allow for large scale production, the expenditure is still substantial due to costs associated with clean rooms, Pt targets, and ultra-high vacuum equipment. In addition, the Pt deposited is often unsupported and the electrolyte cannot be deposited simultaneously with the Pt limiting the catalyst layer to only two dimensions.

Inkjet printing is a technique which is used to transfer liquid phase material onto a substrate in a controlled and non-contact manner. The non-contact is achieved by application of external signal to the printhead. Inkjet printing (IJP) can be used to deposit catalyst materials onto gas diffusion layers (GDLs) that are made into membrane electrode assemblies (MEAs) for polymer electrolyte fuel cell (PEMFC). Existing ink deposition methods such as spray painting or screen printing are not well suited for ultra-low (<0.5 mg Pt cm^{-2}) loadings. The IJP method can be used to deposit smaller volumes of water-based catalyst ink solutions with picolitre precision provided the solution properties are compatible with the cartridge design. Inkjet technology is a commendable tool in many applications including graphics printing, bioengineering and micro-electromechanical systems (MEMS). Droplet stability is a key factor influencing inkjet performance. The stability can be analyzed using dimensionless numbers that usually combine thermophysical properties and system dimensions. In this paper, a drop-on-demand (DOD) inkjet experimental system is established. A numerical model is developed to investigate the influence of the operating conditions on droplet stability, including nozzle dimensions, driving parameters (the pulse amplitude and width used to drive droplet formation) and fluid properties.

Table 2.1 List of papers referred

S. NO	PAPER NAME	AUTHOR NAME	YEAR	EXPERIMENT
1.	Analysis of droplet stability after ejection from an inkjet nozzle	Yonghong Zhong et al.	2018	The droplet stability can be improved by adjusting the pulse amplitude and width, fluid density and viscosity, nozzle diameter and fluid surface tension.
2.	Future, Opportunities and Challenges of Inkjet Technologies	J.R. Castrejon Pita et al.	2013	Future, Opportunities and Challenges of Inkjet Technologies
3.	Inkjet printing of carbon supported platinum 3-D catalyst layers for use in fuel cells	Andr´e D. Taylor et al.	2007	Inkjet printing has been demonstrated as a catalyst application method for PEMFCs.
4.	The roles of wettability and surface tension in droplet formation during inkjet printing	Bing He et al.	2017	The roles of wettability and surface tension controlling the print quality and speed
5.	Optimization of Experimental Parameters to Suppress Nozzle Clogging in Inkjet Printing	Ayoung Lee et al.	2012	The drop jetting for zinc oxide (ZnO) particulate suspensions was studied and optimized
6.	Ink-Jet Printing: A Versatile Method for Multilayer Solid Oxide Fuel Cells Fabrication	Mary A. Sukeshini et al	2009	ink-jet printing has been successfully used to fabricate complete SOFC button cells

7.	Inkjet Printing for Manufacturing Solid Oxide Fuel Cells	Gwon Deok Han et al	2020	To develop high performance solid oxide fuel cells (SOFCs) that can operate at low temperatures use inkjet printing
8.	Influence of Fluid Physical Properties on Ink-Jet Printability	Daehwan Jang et al	2009	The interrelationship between ink-jet printability and the print fluid's physical properties has been studied
9.	Fabrication of polymer electrolyte membrane fuel cell MEAs utilizing inkjet print technology	Silas Towne et al	2007	Fabrication of MEA for PEMFC using commercial inkjet printer
10.	Simulations of microfluidic droplet formation using the two-phase level set method	Shazia Bashir et al	2011	The two-phase level set method, which is ideally suited for tracking the interfaces between two immiscible fluids, has been used to perform numerical simulations of droplet formation in a T-junction.
11.	A Coupled Level Set Projection Method Applied to Ink Jet Simulation	Jiun-Der Yu et al		Developed an axisymmetric second order coupled level set projection method with contact model to model flow in an ink jet printhead, performed numerical simulations to check internal consistency, and compared results with experimental data.

12.	Experimentation modelling and optimization of electrohydrodynamic Inkjet microfabrication approach: a Taguchi regression analysis	Amit Kumar ball et al	2019	The current research work focused on the modelling and optimization of the EHD inkjet printing system. The effects of input process parameters on droplet diameter formation were analysed using Taguchi methodology and regression analysis.
13.	Analysis of drop-on-demand piezo inkjet performance	Seung-Hwan Kang et al	2020	The characteristics and performance of DOD piezoelectric inkjet drops were analysed according to how the liquid's properties changed.
14.	Numerical Modelling of the Motion and Interaction of a Droplet of an Inkjet Printing Process with a Flat Surface	Tim Tofan et al	2021	Droplet ejection, motion, and impact were analysed using the COMSOL CFD module. Numerical experiments were performed on this basis.
15.	Effects of nozzle and fluid properties on the drop formation dynamics in a drop-on-demand inkjet printing	A. B. Aqeel et al	2019	In this study we have conducted systematic Numerical simulations with special efforts on optimizing the contracting angle of the nozzle, the wettability of the inner surface, and the physical properties of the working fluid.
16.	Fabrication of lanthanum strontium cobalt ferrite (LSCF) cathodes for high performance solid	Gwon Deok Han et al	2015	In this study, we successfully fabricated thin film porous LSCF cathodes for SOFCs using the inkjet printing

	oxide fuel cells using a low-price commercial inkjet printer			technique. For fabrication of the LSCF layers, a customized water-based ink source was used, and printing was conducted in a commercial HP printer.
17.	Thermal inkjet printing of thin-film electrolytes and buffering layers for solid oxide fuel cells with improved performance	Chao Li et al	2013	In this work, thin-film YSZ electrolytes and SDC buffering layers were successfully fabricated via an inkjet printing method using a thermal inkjet printer.

2.2 DESCRIPTION

1. In this paper, **the stability of the droplet was numerically and experimentally analysed under different operating conditions** by **Yonghong Zhong (2018)**. The stability can be analysed using dimensionless numbers that usually combine thermophysical properties and system dimensions. In this paper, a drop-on-demand (DOD) inkjet experimental system is established. A numerical model is developed to investigate the influence of the operating conditions on droplet stability, including nozzle dimensions, driving parameters (the pulse amplitude and width used to drive droplet formation) and fluid properties.

2. J.R. Castrejon-Pita (2013) discusses about the **future, opportunities and challenges of Inkjet Technologies** in this paper. Inkjet printing relies on the formation of small liquid droplets to deliver precise amounts of material to a substrate under digital control. Inkjet technology is becoming relatively mature and is of great industrial interest thanks to its flexibility for graphical printing and its potential use in less conventional applications such as additive manufacturing and the production of printed electronics and other functional devices. However, the technology is in need of further development to become mainstream in emerging applications such as additive manufacturing (3D printing).

3. Andr´e D. Taylor (2007) uses a method of **inkjet printing (IJP) to deposit catalyst materials onto gas diffusion layers (GDLs)** that are made into membrane electrode assemblies (MEAs) for polymer electrolyte fuel cell (PEMFC). Existing ink deposition methods such as spray painting or screen printing are not well suited for ultra-low (<0.5 mg Pt cm^{-2}) loadings. The IJP method can be used to deposit smaller volumes of water-based catalyst ink solutions with picolitre precision provided the solution properties are compatible with the cartridge design.

4. This paper by **Bing He (2017)** describes a **lattice Boltzmann-based binary fluid model for inkjet printing**. In this model, a time-dependent driving force is applied to actuate the droplet ejection. As a result, the actuation can be accurately controlled by adjusting the intensity and duration of the positive and negative forces, as well as the idle time. The present model was verified by reproducing the actual single droplet ejection process captured by fast imaging. This model was subsequently used to investigate droplet formation in piezoelectric inkjet printing.

5. Optimization of Experimental Parameters to Suppress Nozzle Clogging in Inkjet Printing by **Ayoung Lee (2012).** Stable drop jet ability is mandatory for a successful, technical scale inkjet printing, and accordingly, this aspect has attracted much attention in fundamental and applied research. Previous studies were mainly focused on Newtonian fluids or polymer solutions. Here, we have investigated the drop jetting for zinc oxide (ZnO) particulate suspensions. Generally, the inverse Ohnesorge number $Z = Oh^{-1}$, which relates viscous forces to inertia and surface tension, is sufficient to predict the jet ability of single-phase fluids.

6. In this work by **Mary A. Sukeshini (2009)**, **ink-jet printing has been successfully used to fabricate complete SOFC button cells** comprised of electrolyte, anode functional, cathode functional, and cathode current collector layers. SEM of the printed layers revealed a dense electrolyte and porous anode interlayer. Cells tested in hydrogen produced a stable voltage of 1.1 V. Cells incorporating a printed anode interlayer, electrolyte but pasted cathode exhibited a maximum power density of 0.30 W/cm^2 at 8001°C. Cells comprised of all layers ink-jet printed exhibited slightly lower performance with 0.21 W/cm^2 at 8001°C.

7. The inkjet printing, which enables precise thin-film production in a simple and cost-effective manner, can have an important role in the implementation of the thin-film SOFC technology. In this study by **Gwon Deok Han (2020)**, **a method to manufacture the entire SOFC using a low-cost commercial inkjet printer** is proposed. All the developed ceramic inks exhibited long-term dispersion stabilities and fluid properties suitable for inkjet printing.

8. Daehwan Jang (2009) discusses the **influence of fluid physical properties on Ink-Jet Printability**. Ink-jet printing is a method for directly patterning and fabricating patterns without the need for masks. To achieve this, the fluids used as inks must have the capability of being stable and accurately printed by ink-jetting. We have investigated the inter-relationship between ink-jet printability and physical fluid properties by monitoring droplet formation dynamics. The printability of the fluids was determined using the inverse (Z) of the Ohnesorge number (Oh) which relates to the viscosity, surface tension, and density of the fluid.

9. Fabrication of polymer electrolyte membrane fuel cell MEAs utilizing inkjet print technology by **Silas Towne (2007).** Utilizing drop-on-demand technology, we have successfully fabricated hydrogen–air polymer electrolyte membrane fuel cells (PEMFC), demonstrated some of the processing advantages of this technology and have demonstrated that the performance is comparable to conventionally fabricated membrane electrode assemblies (MEAs). Commercial desktop inkjet printers were used to deposit the active catalyst electrode layer directly from print cartridges onto Nafion polymer membranes in the hydrogen form. The layers were well-adhered and withstood simple tape peel, bending and abrasion tests and did so without any post-deposition hot press step.

10. Simulations of microfluidic droplet formation using the two-phase level set method by **Shazia Bashir (2011).** The two-phase level set method, which is ideally suited for tracking the interfaces between two immiscible fluids, has been used to perform numerical simulations of droplet formation in a T-junction. Numerical predictions compare well with experimental observations. The influence of parameters such as flow rate ratio, capillary number, viscosity ratio and the interfacial tension between the two immiscible fluids is known to affect the physical processes of droplet generation. In this study the effects of surface wettability, which can be controlled by altering the contact angle, are investigated systematically. As competitive wetting between liquids in a two-phase flow can give rise to erratic flow patterns, it is often desirable to minimize this phenomenon as it can lead to a disruption of the regular production of uniform droplets.

11. A coupled level set projection method applied to ink jet simulation by **Jiun-Der Yu.** A finite difference level set-projection method on rectangular grid is developed for piezoelectric ink jet simulation. The model is based on the Navier-Stokes equations for incompressible two-phase flows in the presence of surface tension and density jump across the interface separating ink and air, coupled to an electric circuit model which describes the driving mechanism behind the process, and a macroscopic contact model which describes the air-ink-wall dynamics.

12. Experimentation modelling and optimization of electrohydrodynamic inkjet microfabrication approach: a Taguchi regression analysis by **Amit Kumar ball (2019).** Electrohydrodynamic (EHD) inkjet is a modern non-contact printing approach, which uses a direct writing technology of functional materials to achieve micro/nanoscale of printing resolution. As an alternative to conventional inkjet technology, the goal of the EHD inkjet printing is to generate uniformly minimized droplets on a substrate. In this study, the effects of applied voltage, standoff height and ink flow rate on droplet diameter formation in EHD inkjet printing process were analysed using Taguchi methodology and regression analysis.

13. Analysis of drop-on-demand piezo inkjet performance by **Seung-Hwan Kang (2020).** The characteristics and performance of DOD piezoelectric inkjet drops were analysed according to how the liquid's properties changed. An experimental ink was made of an aqueous solution of polyethylene glycol which had particular properties. As the temperature decreased, the ink's viscosity and surface tension increased; which in turn causes Oh to increase and Z to decrease. Oh and Z are dimensionless numbers that are often used to characterize ink in these kinds of experiments.

14. Numerical Modelling of the Motion and Interaction of a Droplet of an Inkjet Printing Process with a Flat Surface by **Tim Tofan (2021).** The numerical simulation and analysis of the ejection of an ink droplet through a nozzle as well its motion through air until its contact with a surface and taking up of a stable form is performed. The fluid flow is modelled by the incompressible Navier–stokes equations with added surface tension. The presented model can be solved using either a level set or a phase field method to track the fluid interface. Here, the level set method is used to determinate the interface between ink and air.

15. Effects of nozzle and fluid properties on the drop formation dynamics in a drop-on-demand inkjet printing by **A.B. Aqeel (2019).** The droplet formation dynamics of a Newtonian liquid in a drop-on-demand (DOD) inkjet process is numerically investigated by using a volume-of-fluid (VOF) method. We focus on the nozzle geometry, wettability of the interior surface, and the fluid properties to achieve the stable droplet formation with higher velocity. It is found that a nozzle with contracting angle of 45° generates the most stable and fastest single droplet, which is beneficial for the enhanced printing quality and high-throughput printing rate.

16. Fabrication of lanthanum strontium cobalt ferrite (LSCF) cathodes for high performance solid oxide fuel cells using a low-price commercial inkjet printer by **Gwon Deok Han (2015).** In this study, we investigate a method to fabricate high quality lanthanum strontium cobalt ferrite (LSCF) cathodes for solid oxide fuel cells (SOFCs) using a commercial low price inkjet printer. The ink source is synthesized by dissolving the LSCF nano powder in a water-based solvent with a proper amount of surfactants. Microstructures of the LSCF layer, including porosity and thickness per printing scan cycle, are adjusted by grayscale in the printing image. It is successfully demonstrated that anode-supported SOFCs with optimally printed LSCF cathodes can produce decent power output.

17. Thermal inkjet printing of thin-film electrolytes and buffering layers for solid oxide fuel cells with improved performance by **Chao Li (2013).** In this work, thin-film YSZ electrolytes and SDC buffering layers were successfully fabricated via an inkjet printing method using a thermal inkjet printer. Well-dispersed aqueous inks with high solid loads were prepared for inkjet printing. The Z values of the prepared inks fit well within the printable range. For the printed YSZ electrolyte, the SEM photos indicated that a single printing resulted in a membrane thickness of approximately 1.5 mm. Cells with YSZ layers printed with 4 repetitions and with a sprayed LSM cathode produced an OCV of approximately 1.05 V and a PPD of 860 mW/cm^2 at 800 °C.

CHAPTER 3

OBJECTIVES

Major objectives are

- To learn the basics of COMSOL (Analysis Software) version 5.5 and study about Level Set Method.
- To design an initial inkjet nozzle for Membrane Electrode Assembly (Fuel Cell) to print the catalyst (gaseous layer).
- To identify the key parameters involved in designing the nozzle for Membrane Electrode Assembly.
- To identify the relation between those key parameters and mass of droplet formed to optimize the nozzle.
- To optimize the nozzle design for Membrane Electrode Assembly based on the obtained results and some standard methods (Example – Taguchi method, Genetic Algorithm).

CHAPTER 4

SOFTWARE USED FOR ANALYSIS

COMSOL software has been used to study and optimize the parameters of the inkjet printer nozzle for fuel cell application.

4.1 COMSOL

COMSOL Multiphysics is a cross-platform finite element analysis, solver, and multiphysics simulation software. It allows conventional physics-based user interfaces and paired systems of partial differential equations (PDEs). COMSOL provides an IDE and unified workflow for electrical, mechanical, fluid, acoustics, and chemical applications.

Besides the classical problems which will be addressed with application modules, the core Multiphysics package are often wont to solve PDEs (Partial Differential Equation) in weak form. An API for Java and a live link for MATLAB and Autodesk Inventor could also be wont to control the software externally. An Application Builder are often wont to develop independent custom domain-specific simulation applications. Users may use drag-and-drop tools (Form Editor) or programming (Method Editor). COMSOL Server is a distinct software for the management of COMSOL simulation applications in companies. Several modules are available for COMSOL, categorized consistent with the applications areas of Electrical, Mechanical, Fluid, Acoustic, Chemical, Multipurpose, and Interfacing.

Figure 4.1 COMSOL Software logo

4.2 WHY COMSOL

We are using COMSOL version 5.5 as we can readily set up the model using the Laminar Two-Phase Flow, Level Set interface. This interface adds the equations automatically, and we need to specify only the physical parameters of the fluids and the initial and boundary conditions.

To accurately resolve the interface between the air and ink we can use adaptive meshing. This means that as the interface moves during the simulation, the mesh gets updated to keep the mesh refined in the interface region. The simulation procedure involves two consecutive computations. First, we calculate a smooth initial solution for the level set variable. Using this initial solution, we then start the time-dependent simulation of the fluid motion.

It takes low temporary memory (RAM) and the user interface is easy to understand. The time taken to solve iterations is less when compared to other software.

4.3 BENEFITS OF USING COMSOL

- General-purpose simulation software based on advanced numerical methods.
- Fully coupled multiphysics and single-physics modelling capabilities.
- Complete modelling workflow, from geometry to post-processing.
- User-friendly tools for building and deploying simulation apps.

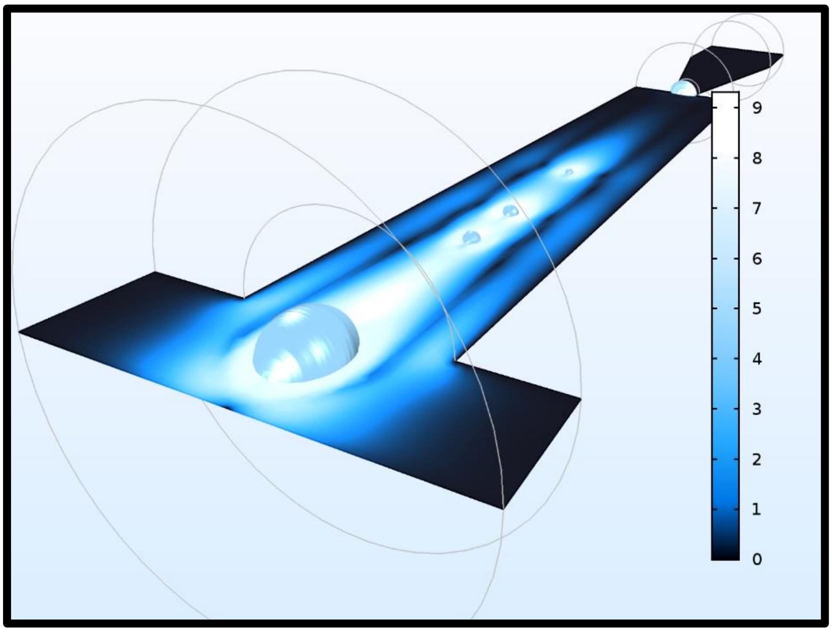

Figure 4.2 Droplet Simulation in COMSOL

CHAPTER 5

LEVEL SET METHOD

5.1 MODEL DEFENITION

The nozzle because example. Because of its symmetry we can use an axisymmetric 2D model. Initially, the space between inlet and nozzle is filled with ink. Additionally, more ink is injected through inlet during required time period and it consequently forces ink to flow out of the nozzle. When the injection stops, a droplet of ink forces out and continues to travel until it hits the target. The flow is two phase and laminar.

5.2 REPRESENTATION OF FLUID INTERFACE – LEVEL SET METHOD

Fluid flow with moving interfaces or boundaries occur in different applications, such as fluid-structure interaction, multiphase flows, and flexible membranes moving in a liquid. One way to solve moving interfaces is to use a level set method. A certain contour line of a globally defined function, the level set function, then represents the interface between phases. With the Level Set modelling interface, we can move the fluid-fluid interface within any velocity field. The level set method is a technique to represent moving interfaces or boundaries using a fixed mesh. It is useful for problems where the computational domain is divided into two domains separated by an interface. Each of the two domains may have consist of several parts. The interface is represented by a certain level set or isocontour of the globally defined function, the level set function **ϕ**. In COMSOL Multiphysics, **ϕ** is a smooth step function that equals zero in a domain and one in the other. Across the interface, there is a smooth transition from zero to one. The interface is defined by the 0.5 isocontour, or the level set, of **ϕ.**

The Laminar Two-Phase Flow, Level Set interface uses a reinitialized, conservative level set method to describe and convect with the fluid interface. The 0.5 contour of the level set function defines the interface, where equals 0 for air and 1 for ink. In a transition layer which is close to the interface, the value goes smoothly from 0 to 1. The interface moves with the fluid velocity, u, at the interface.

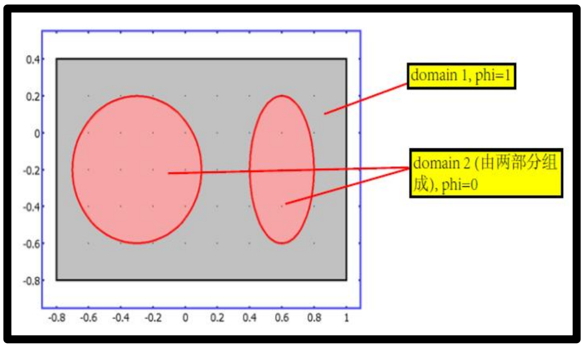

Figure 5.1 Example of domains

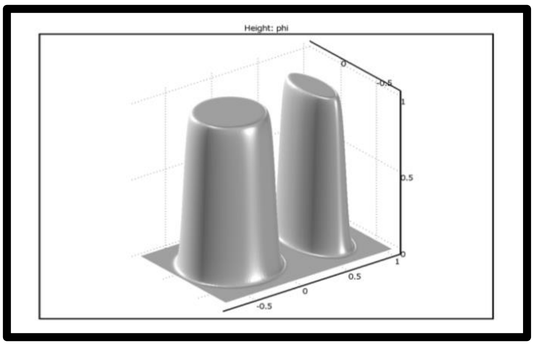

Figure 5.2 surface plot of function

The modelling interface solves the following equation in order to move the interface with the velocity field u:

$$\frac{\partial \phi}{\partial t} + \mathbf{u} \cdot \nabla \phi = \gamma \nabla \cdot \left(\varepsilon \nabla \phi - \phi(1 - \phi) \frac{\nabla \phi}{|\nabla \phi|} \right)$$

The left-hand side of the equation give the correct motion of the interface, while those on the right-hand side are necessary for numerical stability. The parameter, Ɛ, determines the thickness of the region where goes smoothly from zero to one and is normally of the same order as the size of the elements of the mesh. ɣ is constant within each domain and equals the largest value of the mesh size, h, within the domain. The parameter Ɛ determines the amount of reinitialization or stabilization of the level set function. It needs to be modified for each specific problem. If Ɛ is too small, the thickness of the interface may not remain constant, and oscillations may appear because of numerical instabilities. On the other hand, if Ɛ is too large, the interface moves incorrectly. A suitable value for Ɛ is the maximum magnitude of the velocity field u.

5.3 CONSERVATIVE AND NON-CONSERVATIVE FORM

If the velocity is divergence free, that is, if

$$\nabla \cdot \mathbf{u} = 0$$

the volume (area for 2D problems) bounded by the interface is said to be conserved if there is no inflow or outflow through the boundaries. To obtain exact numerical conservation, we can change to the conservative form

$$\frac{\partial \phi}{\partial t} + \nabla \cdot (\mathbf{u}\phi) = \gamma \nabla \cdot \left(\varepsilon \nabla \phi - \phi(1-\phi)\frac{\nabla \phi}{|\nabla \phi|} \right)$$

In the Level Set feature's Settings window. Using the conservative level set form, we obtain exact numerical conservation of the integral of **ϕ**. Note, however, that the non-conservative form is considered to be more suited for numerical calculations and usually converges more easily. The non-conservative form, which is the default form, only conserves the integral of the level set function approximately, but this is considered sufficient for most applications.

5.4 INITIALISING THE LEVEL SET FUNCTION

Before we can solve Equation, we should initialize the level set function such that it varies smoothly from zero to one across the interface. Do so by letting be zero on one side of the interface and one on the other. Then solve using this as the initial condition. The resulting is smooth across the interface and a suitable initial condition to the level set equation. The Level Set interface automatically sets up Equation if we select Transient with Initialization from the Studies list in the Select Study Type page when adding the physics interface.

5.5 THE LEVEL SET INTERFACE

The Level Set interface provides the equations and boundary conditions for using the level set method to track moving interfaces in fluid-flow models, solving for the level set function. The main feature is the Model Settings feature, which adds the level set equation and provides an interface for defining the level set properties and the velocity field. We find the Level Set interface in the Mathematics > Moving Mesh folder on the Add Physics page in the Model Wizard. When we add the Level Set interface, it creates the Level Set node with default Model Settings and No Flow (the default boundary condition) nodes added. There is also a default Initial Values feature. Right-click the Level Set node to add other boundary conditions, for example. The following sections provide information about all feature nodes available in the Level Set interface. The level set window contains the following sections

- Interface identifier
- Domains
- Stabilization
- Advanced settings
- Discretization
- Dependent variables

5.5.1 INTERFACE IDENTIFIER

This is the identifier for the interface, which we use to reach the fields and variables in expressions, for example. The identifier appears in the Identifier edit field, and we can change it to any unique string that is a valid identifier. The default identifier (for the first Level Set interface in the model) is **ls**.

5.5.2 DOMAINS

In this section we select the domains where we want to define the level set function and the level set equation that describes it. The default setting is to include all domains in the model.

5.5.3 STABILIZATION

To display this section, select Show More Options from the View menu in the Model Builder.

This section contains settings for the stabilization methods. There are two types of stabilization methods for the level set equation: streamline diffusion and crosswind diffusion. Both are active per default and should remain active for optimal performance. To disable one or both of the stabilization methods, clear either or both of the Streamline diffusion and Crosswind diffusion check boxes.

5.5.4 ADVANCED SETTINGS

To display this section, select Show More Options from the View menu in the Model Builder. In this section we can specify some advanced settings that we normally do not need to change. This section has three parts

- Convective terms

- Equation form
- Show all model inputs

5.5.5 DISCRETIZATION

To display this section, select Show More Options from the View menu in the Model Builder. In this section we can specify the order of the shape functions. The default is to use second-order Lagrange elements.

5.5.6 DEPENDENT VARIABLES

Here we can change the name of the dependent variable for the volume fraction of the fluid. To change the name, type a new name in the Volume fraction of fluid 2 edit field

5.6 MODEL SETTINGS

The Model Settings feature provides the possibility to define the associated level set parameters and the velocity field. The Model Settings window contains the following sections

- Domains
- Level set parameters
- Convection

5.7 INITIAL VALUES

The Initial Values feature adds an initial value for the level set function that can serve as an initial condition for a transient simulation. If we need to specify more than one set of initial values, we can add additional Initial Values features. The Initial Values window contains the following sections:

- DOMAINS
- INITIAL VALUES

5.8 BOUNDARY CONDITIONS

We do not need to specify a boundary condition for axial symmetry. The Level Set interface contains the following boundary conditions:

- Initial Interface
- Inlet
- No Flow (the default boundary condition)

- Outlet
- Symmetry

5.8.1 INITIAL INTERFACE

The Initial Interface feature defines the boundary as the initial position of the interface.

5.8.2 INLET

The Inlet feature adds a boundary condition for inlets (inflow boundaries) in a Level Set interface. At inlets we should specify a value of the level set function Typically we set to either 0 or 1.

5.8.3 NO FLOW

The No Flow feature adds a boundary condition that represents boundaries where there is no flow across the boundary. This is the default boundary condition.

5.8.4 OUTLET

The Outlet feature adds a boundary condition for outlets (outflow boundaries) in a Level Set interface. This feature imposes no boundary condition on the level set function.

5.8.5 SYMMETRY

The Symmetry feature adds a boundary condition for boundaries that represent a symmetry line or symmetry plane. For the symmetry axis at $r = 0$, the program automatically provides a suitable boundary condition and adds an Axial Symmetry feature to the model that is valid on the axial symmetry boundaries only.

CHAPTER 6

ANALYSIS AND TESTING

6.1. INTRODUCTION

To create an optimized inkjet nozzle design for Membrane Electrode Assembly (Fuel Cell) to print the catalyst (gaseous layer). The parameters of the nozzle design have to be optimized to precisely get the required mass of catalyst in a certain amount of time. We create an initial design based on the industrial standards and then the design is optimized for the required quantity.

6.2. NOZZLE DESIGN

The droplet size for an inkjet nozzle is a key design parameter. To produce the desired size, optimizing the design of the nozzle and the inkjet's operating conditions is key. We use a Drop on Demand inkjet printer for our application and the basic industry standard for the diameter of the nozzle is 20-50μm (same as the droplet size). The convergent nozzle has been divided into several parts to make the analysis much more efficient. The nozzle parameters include inlet radius, outlet radius, length of the nozzle. The inlet radius and the length of the nozzle are selected concerning the diameter of the nozzle.

Also, the droplet from the nozzle tip to the point where it reaches the endplate has to be analyzed so we get the desired time results for the application, so we create a flow field (two-phase) for it along with its dimensions. Since the entire geometry is axis-symmetric, we use the 2d axis-symmetric FEM method and analyze the inkjet nozzle. Based on standard parameters and assumptions we build a nozzle design from which we start to analyze, vary the parameters and study the effect of change in parameters to the desired result and optimize it according to our application. We have the interface between the ink and air, which involves two-phase mixing and the flow is considered as laminar flow based on the input speed of ink injection so, we use a laminar two-phase model, level set interface to simulate the inkjet nozzle. The simulation procedure involves two consecutive computations. We calculate a smooth initial solution for the level set variable. Using this initial solution, we then start the time-dependent simulation of the fluid motion. So, based on the results the design is modified and reanalyzed**.**

We demonstrate the model of the fluid flow of an inkjet nozzle, for instance, in a printer. An ink droplet is ejected through the nozzle and travels through air until it hits the target. The fluid flow is modeled by the incompressible Navier-Stokes equations with surface tension. The model can be solved using either a level set or a phase field method to track the fluid interface; here we use the level set method. The model also makes use of adaptive meshing.

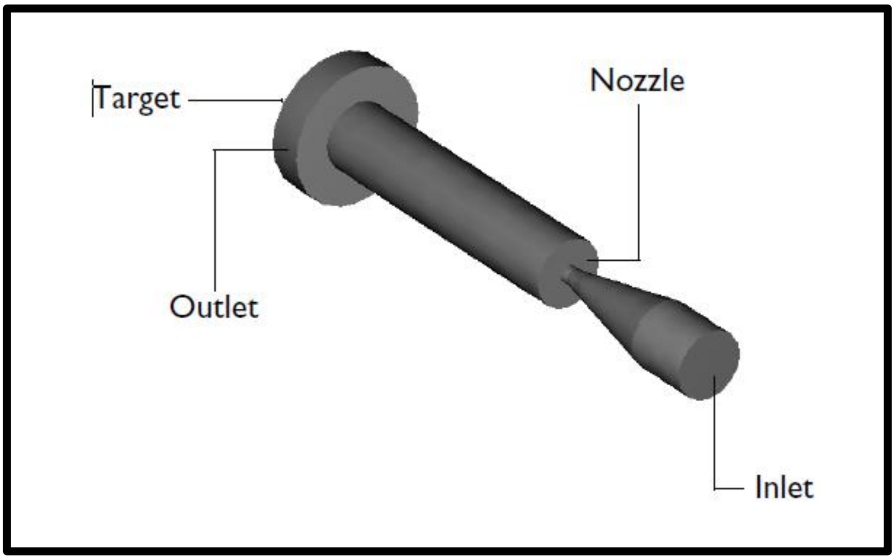

Figure 6.1 Nozzle isometric view

6.3. INITIAL ITERATION

The geometry for the nozzle is to be created in the COMSOL software, so the parameters are defined as global parameters with the keywords. Then the geometry is created as a 2d plane using rectangles and polygon in the drop-down menu by defining the geometry part parameters using the keywords defined globally and it is built. The flow field is also built with the nozzle itself.

The nozzle has the following parts.

1. Inlet chamber
2. Converging nozzle
3. Throat
4. Flow field (Air Chamber)
5. Endplate

Next, we do the form union operation where the individually created parts of the nozzle are made together using this. Now the geometry is complete with defined edges.

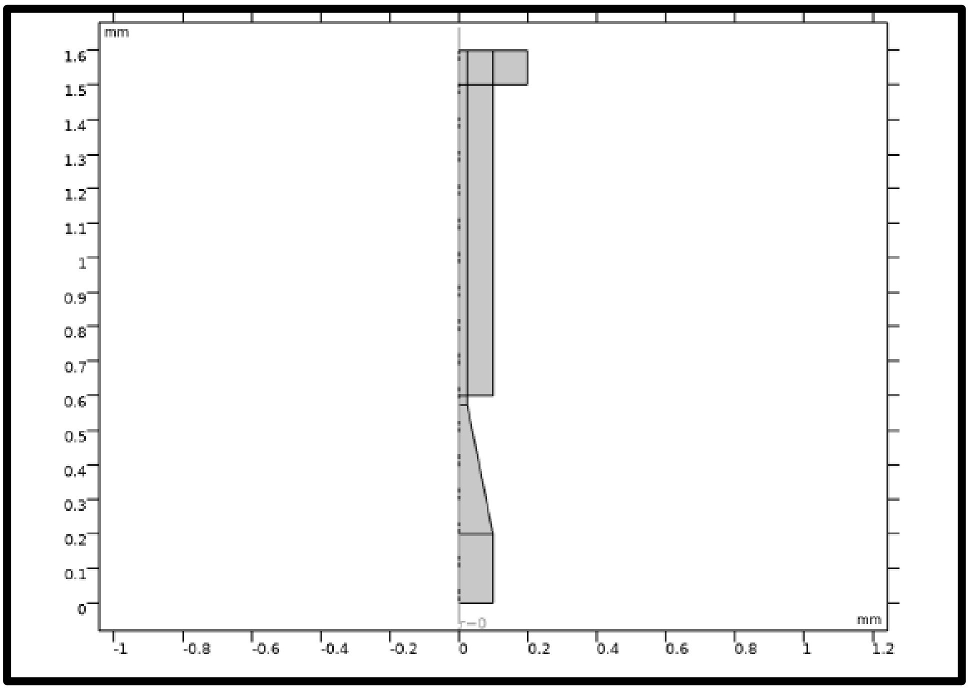

Figure 6.2 2d Axis symmetric design

We have to define the materials that are to be used in the nozzle i.e., ink and air. Ink is the catalyst mixture that is to be fed into the nozzle but since we do initial testing, we use industry-grade ink to study the effect and, in the chamber, the air properties are to be defined. The properties that are fed are density and dynamic viscosity of the ink and air is added from the library of the software.

Boundary conditions for the given nozzle application are taken from the rectangular function that is to be defined. The inlet velocity in the z-direction increases from 0 to the parabolic profile. The inlet velocity and the rectangular function are collectively taken to define the time function for the inkjet nozzle application. The functions are

$$v\ (r,\ t) = rect(t).\ v(r)$$

We use φ=1 as the inlet boundary condition for the level set variable. Constant pressure is set at the outlet. The value of the pressure is not important because the velocity depends only on the pressure gradient.

Thus, we obtain the same velocity field regardless of whether the pressure is set to 1 atm or 0. On all other boundaries except the target, we set No-slip conditions. We use the Wetted wall condition on the target, with a contact angle of π/2 and a slip length of 10 μm.

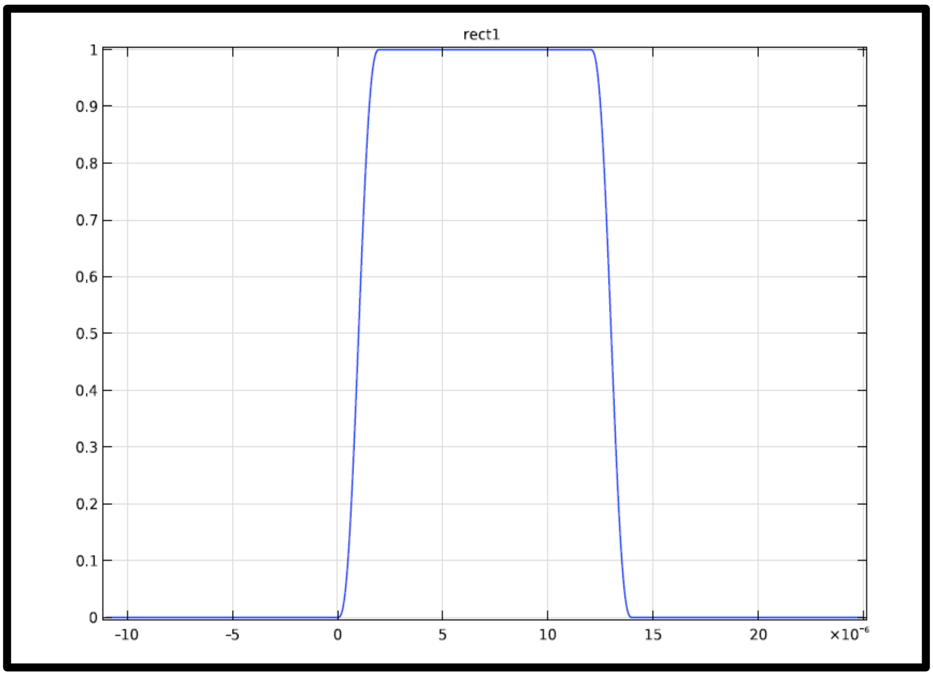

Figure 6.3 Rectangular step function

The rectangular function is defined using the functions option, the lower limit and the upper limit of the function are defined in the parameters section and the smoothing of the curve is carried out.

Next, we carry out integration by defining variable functions for inlet velocity and mass of the droplet.

v_in= 0.56[m/s] *rect1(t[1/s])

The Two-phase, Level set method is activated in the software and the surface tension of the inkjet fluid in the momentum equation is switched on and the value for surface tension coefficient is added.

The flow in the inlet is defined as fully developed flow and the average inlet velocity value is given as v_in (inlet velocity defined). Outlet boundary is selected. εls text field γ text field values are entered. Fluid two domains are defined. Then the wet walls are defined and the total geometry has been meshed and we obtain the final meshed geometry.

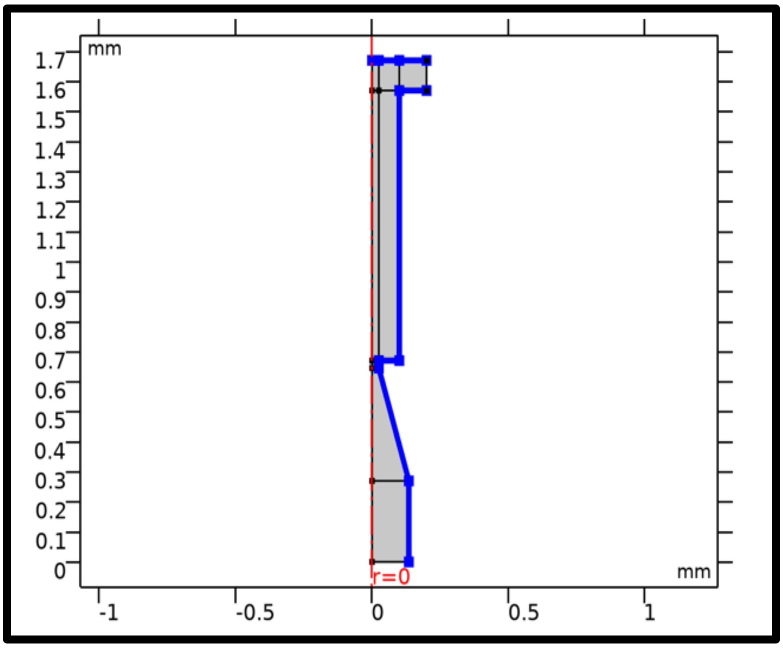

Figure 6.4 Wetted wall selection

We have to study the time-dependent solution for the problem, so the range of time is given as input generally we provide 0 to 200µs with a step size of 10µs. Also, the adaptive mesh function is used. We solve the geometry with inlet velocity as the dependent variable and we obtain the necessary mass vs time graph.

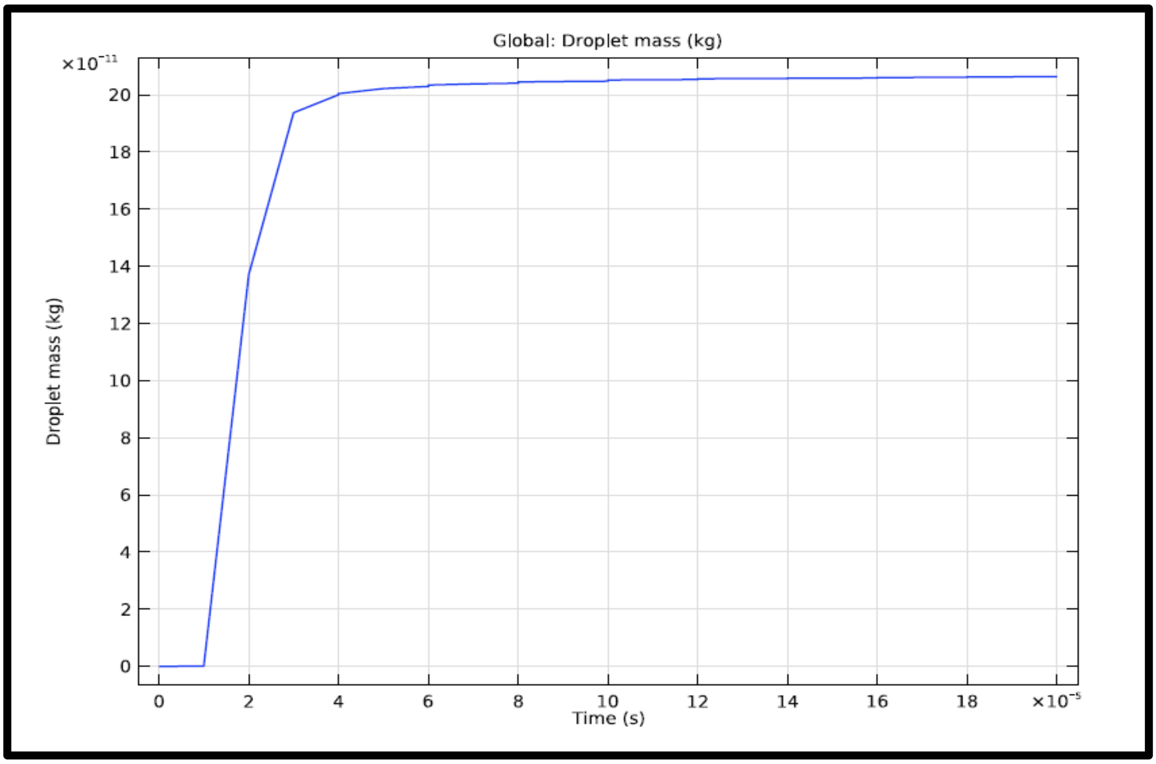

Figure 6.5 droplet mass vs time graph

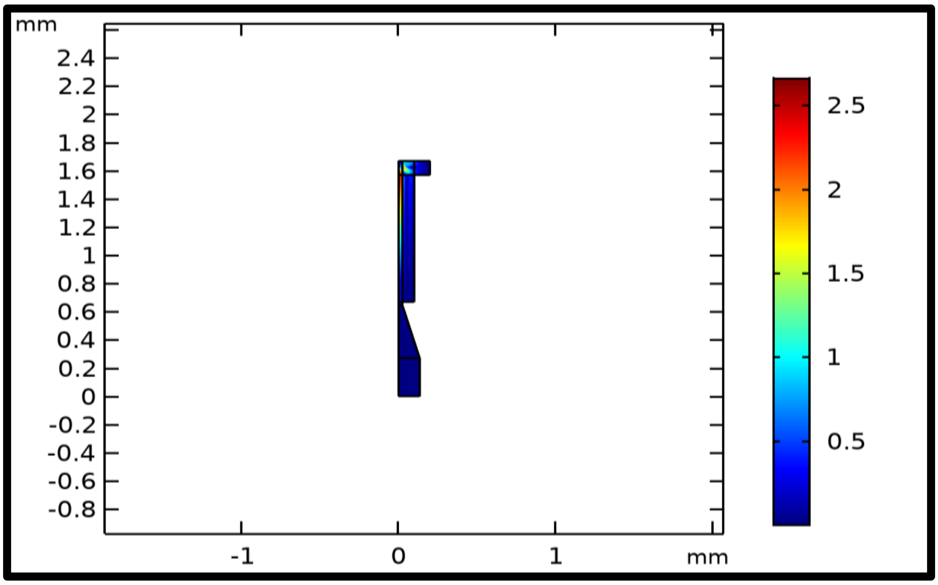

Figure 6.6 Velocity profile

From the above graph, we obtain the value of mass as 20×10^{-11} kg approximately and in 2.5×10^{-5} seconds. So, based on the required values we can optimize the parameters and obtain them. Next, we carry out the study of the effect of parameters in the inkjet nozzle and get the desired combination for the output required. The variation of droplet start time and end time also to be considered for precise printing of the catalyst.

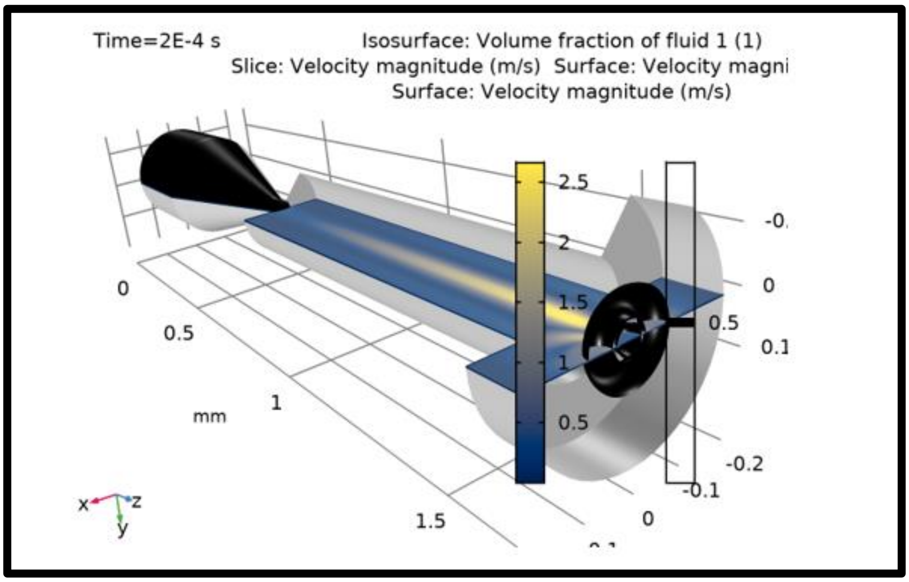

Figure 6.7 Droplet simulation

6.4. PARAMETERS VARIATION

After the initial iteration and results, we identified some of the key parameters that can be varied to optimize the mass flow rate of the nozzle. We will study the effect of the change of these parameters and find the optimal one. The key parameters are **Nozzle Radius, Nozzle Length, Inlet Radius, Air gap width, Inlet velocity of the ink, Density of the ink.**

After identifying the key parameters, we try to find the relation between the key parameters and droplet mass (mass of droplet formed in an inkjet printer), start time (time at which droplet starts to form) by the trial-and-error method. To find the relation of one parameter we keep all other parameters fixed and vary the one parameter.

We follow the same steps as of the initial iteration for the other parameter variation all the boundary conditions and only the geometry is varied according to the parameter varied. Changes in the time domain are done if the flow is not captured in the given standard time domain.

6.4.1. NOZZLE RADIUS

The nozzle radius is the most important parameter for drop formation which also governs the amount of mass coming out of the nozzle. We vary the nozzle radius below and above the initial iteration. The results of parameter varied iterations:

Table 6.1 Nozzle Radius Variation results

S. No	Parameter (in mm)	Start time	Remarks	Peak mass value
1.	0.01	0	Gets to peak and reaches TargetL at time 5 x 10^-5	$21x10^{-11}$
2.	0.02	0	Droplet formation time has decreased	$21x10^{-11}$
3.	0.025	$1x10^{-5}$	Normal value	$20x10^{-11}$
4.	0.03	$1x10^{-5}$	The Increase in droplet formation time and mass of droplet has decreased	$19.2x10^{-11}$
5.	0.05	0	Starts at 0 and becomes -ve i.e the droplet does not come out	0

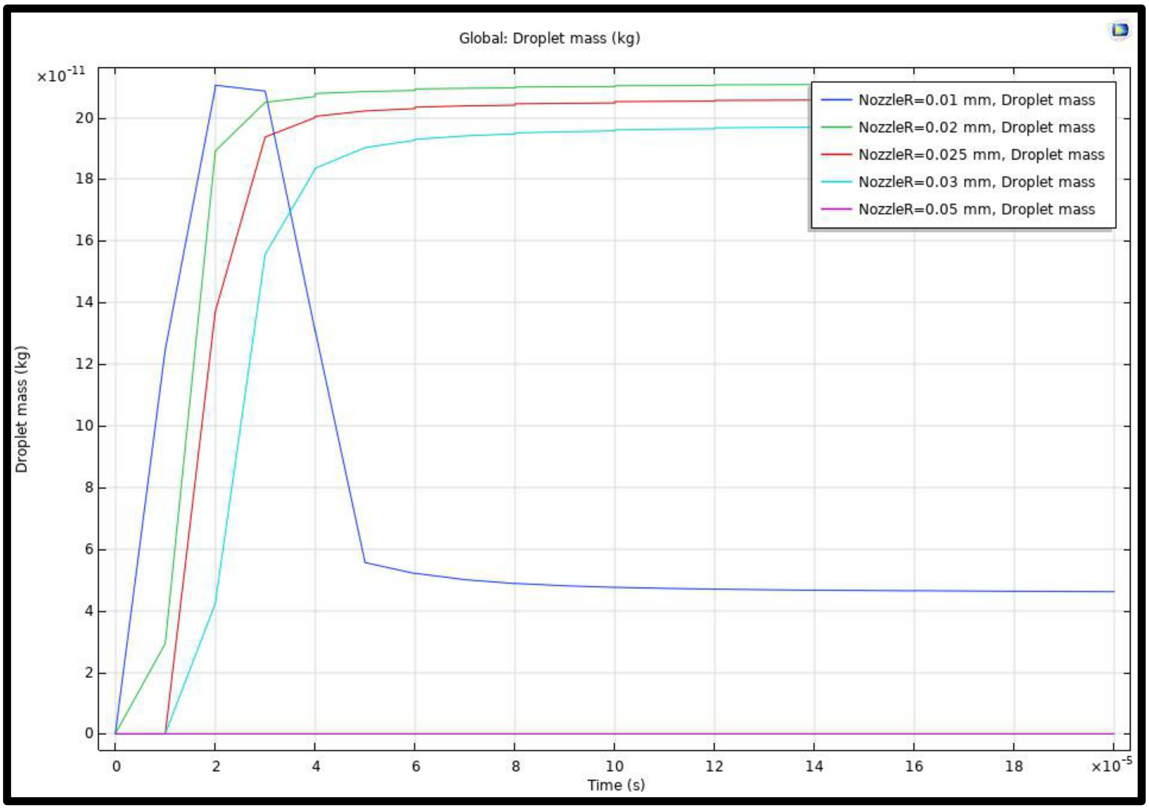

Figure 6.8 Mass vs Time graph (Nozzle radius)

We can conclude from the above data that the mass of the droplet is more or less independent of the size of the inlet radius, but when it exceeds 0.05 the formation doesn't occur. So, we conclude that the nozzle radius is already in the optimized size.

6.4.2. INLET RADIUS

The inlet governs the amount of ink entering the nozzle, so we study how the size of the inlet changes the mass of the droplet and the time of the droplet. The iteration is carried out and the results are tabulated:

Table 6.2 Inlet Radius Variation results

S. No	Parameter (in mm)	Start time	Remarks	Peak mass value
1.	0.075	$3x10^{-5}$	Decrease in the mass of droplet and increase in droplet formation time	$10x10^{-11}$
2.	0.09	$1x10^{-5}$	The peak mass of droplet value decreases	$16x10^{-11}$
3.	0.1	$1x10^{-5}$	Normal value	$20x10^{-11}$

4.	0.125	0	Increase in mass of droplet and decrease in droplet formation time	$33x10^{-11}$
5.	0.15	0	Increase in mass of droplet and decrease in droplet formation time	$47x10^{-11}$

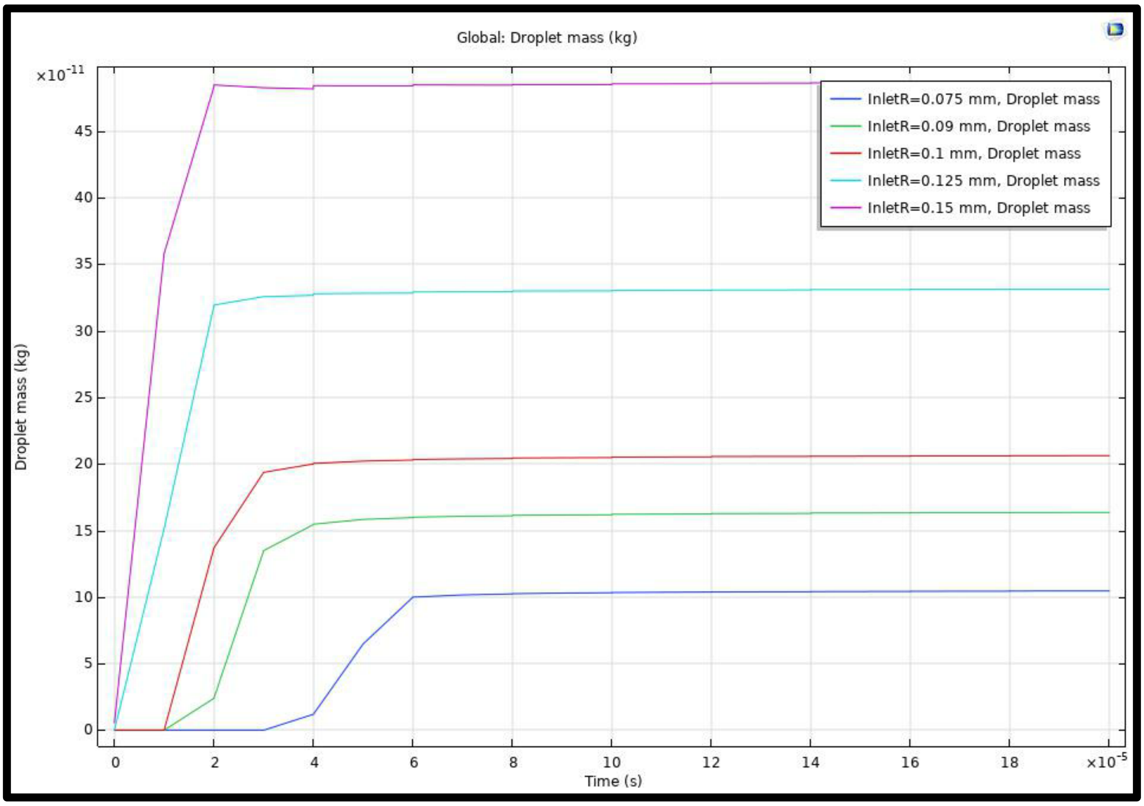

Figure 6.9 Mass vs Time graph (Inlet radius)

We get to a conclusion that the Inlet radius is directly proportional to mass value and inversely proportional to the start time and droplet completion time. So, we obtain a direct relationship from the iteration that is carried out, so based on the requirement the size can be selected.

6.4.3. NOZZLE LENGTH

The nozzle length determines the angle of the nozzle which also is one of the key elements in the ink injection process, the convergence also determines the time of the droplet that travels in the air gap that is defined.

On iterations we found that, the Nozzle length is directly proportional to mass value and inversely proportional to the start time and droplet completion time. So, we obtain a direct relationship from the iteration that is carried out, so based on the requirement the size can be selected. The iteration results are as follows

Table 6.3 Nozzle Length Variation results

S. No	Parameter (in mm)	Start time	Remarks	Peak mass value
1.	0.125	$4x10^{-5}$	Mass of droplet is more or less the same and start time increases	$20x10^{-11}$
2.	0.25	$2x10^{-5}$	Mass of droplet is more or less the same and start time increases	$20x10^{-11}$
3.	0.375	$1x10^{-5}$	Normal value	$20x10^{-11}$
4.	0.5	0	Mass of droplet increases and peak time decreases	$26 \text{ x } 10^{-11}$
5.	0.625	0	Mass of droplet increases and peak time decreases	$6.9x10^{-10}$

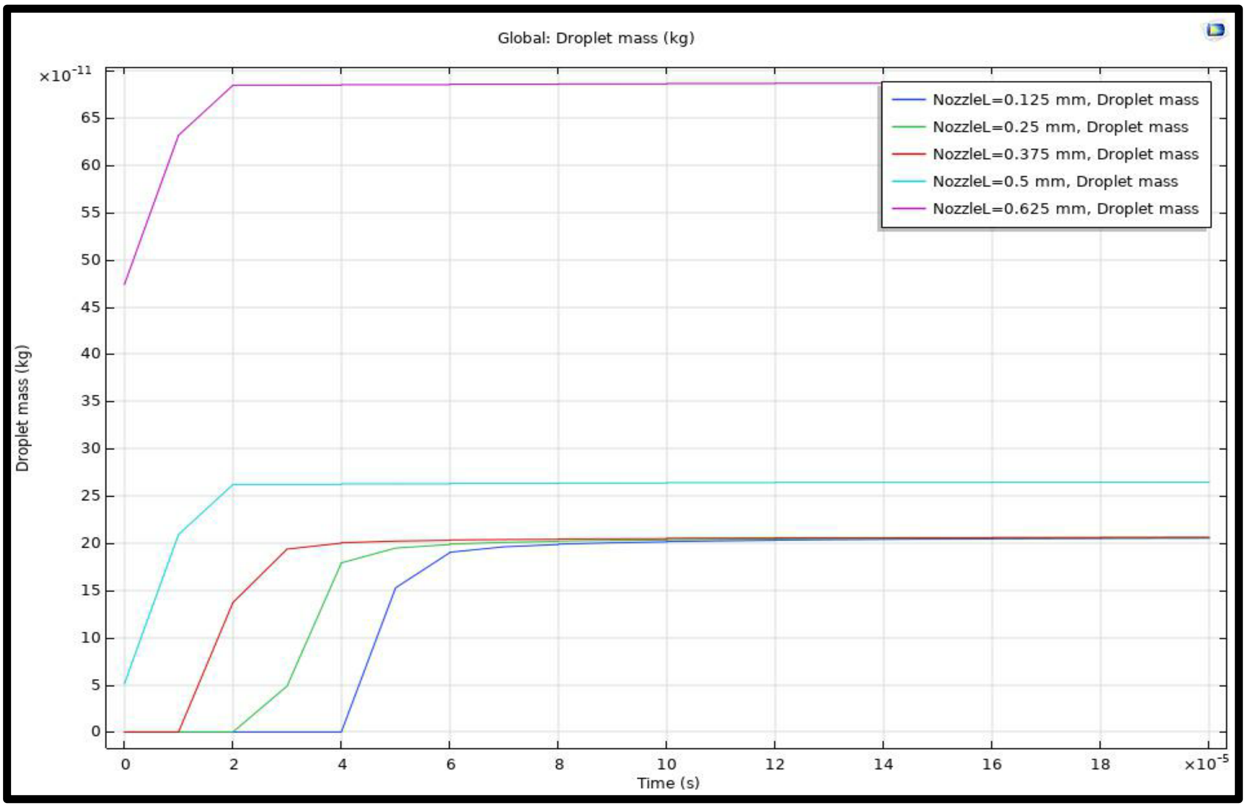

Figure 6.10 Mass vs Time graph (Nozzle length)

6.4.4. AIR WIDTH

Air width is the diameter of the gap between the throat and the target endplate. The width of it tells the amount of air present and pressure gradient, the variation due to these can be studied, the results are tabulated below:

Table 6.4 Air Width Variation results

S. No	Parameter (in mm)	Start time	Remarks	Peak mass value
1.	0.05	$1x10^{-5}$	Start time remains the same, End time increases, a very slight decrease in mass of the droplet	$20.5x10^{-11}$
2.	0.1	$1x10^{-5}$	Normal value	$21x10^{-11}$
3.	0.2	$1x10^{-5}$	End time decreases, same start time, a very slight increase in mass of the droplet	$21.5x10^{-11}$

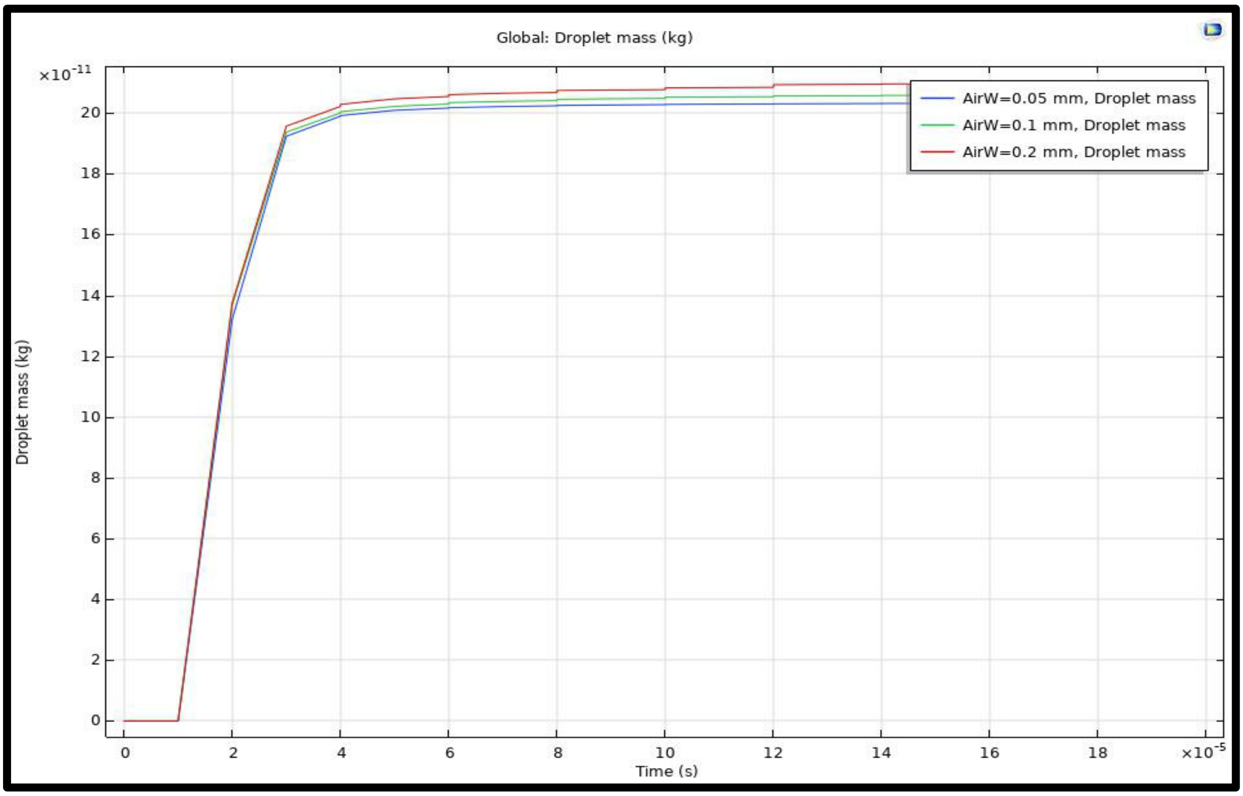

Figure 6.11 Mass vs Time graph (Nozzle radius)

6.4.5. VELOCITY

Inlet Velocity is the velocity at which the ink is fed into the inlet of the nozzle, the variation of the speed concerning the mass of the droplet is analyzed and the result is tabulated:

Table 6.5 Velocity Variation results

S. No	Parameter (in m/s)	Start time	Remarks	Peak mass value
1.	0.25	$2x10^{-5}$	Start time increases, End time also increases, and the mass of the droplet decreases	$80x10^{-12}$
2.	0.56	$1x10^{-5}$	Normal value	$21x10^{-11}$
3.	0.75	0	Start time decreases, End time decreases and Mass of droplet slightly increases	$28x10^{-11}$
4.	1	0	Start time decreases, End time decreases and Mass of droplet slightly increases	$39x10^{-11}$

Based on the results we get to a conclusion that the Velocity is directly proportional to the mass of the droplet and inversely proportional to the time of formation of the droplet.

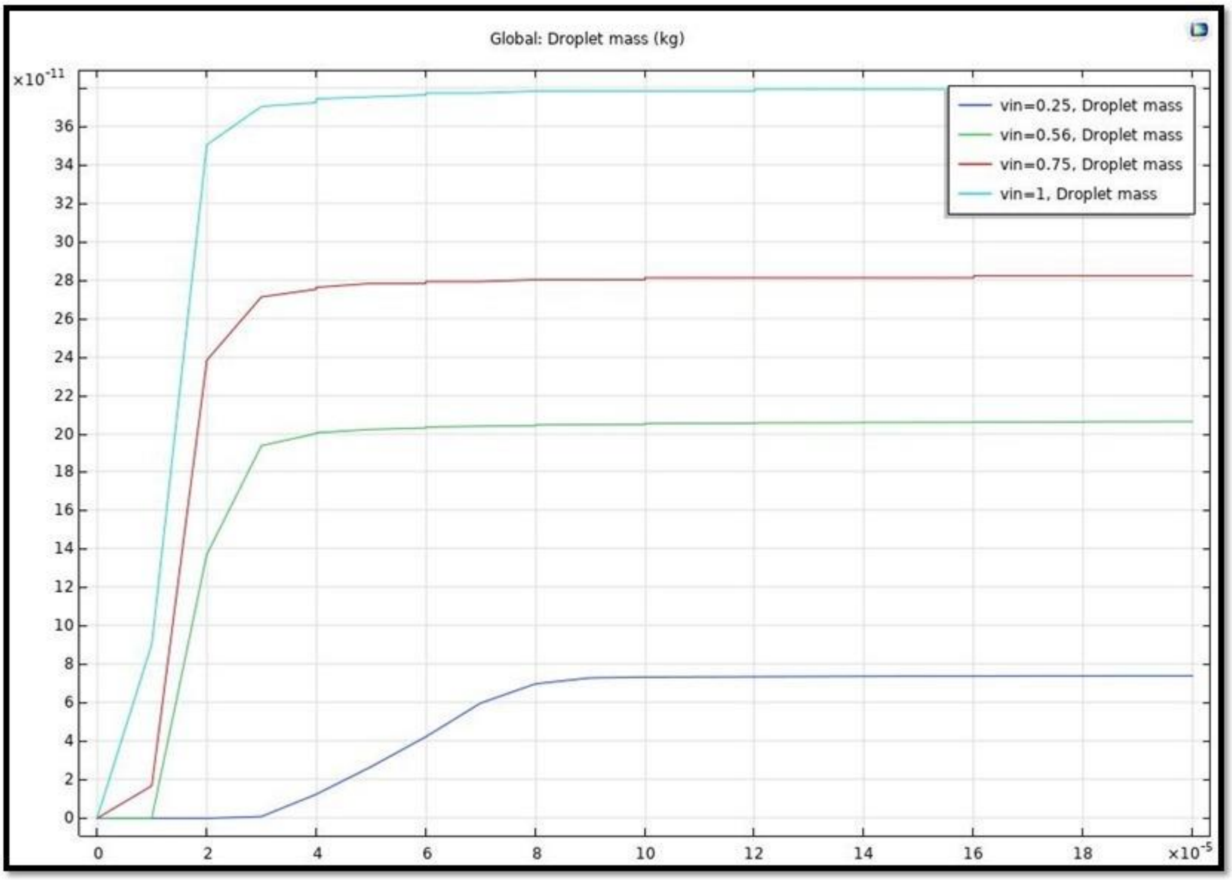

Figure 6.12 Mass vs Time graph (Inlet velocity)

CHAPTER 7

CONCLUSION AND FUTURE SCOPE

In our work, some of the key parameters were varied to optimize the mass flow rate of the nozzle. The effects of the change of these parameters were found. The key parameters are Nozzle Radius, Nozzle Length, Inlet Radius, Air gap width, Inlet velocity of the ink, Density of the ink.

Based on the results obtained by varying parameters of nozzle, we found that the mass flow rate has been dependent on the nozzle parameters and the relationship with these parameters was found by plotting the graphs for these change in parameters.

Keeping the proposed work as base many other new feats can be derived one such proposed work for inkjet nozzle is optimization of nozzle for a specific application using some optimization techniques. There are many optimization techniques, here we give brief introduction two main optimization techniques namely genetic algorithm technique and taguchi method

7.1 GENETIC ALGORITHM

The genetic algorithm is a random-based classical evolutionary algorithm. By random here we mean that in order to find a solution using the GA, random changes applied to the current solutions to generate new ones. GA is based on Darwin's theory of evolution. It is a slow gradual process that works by making changes to the making slight and slow changes. Also, GA makes slight changes to its solutions slowly until getting the best solution.

Genetic algorithms are commonly used to generate high-quality solutions to optimization and search problems by relying on biologically inspired operators such as mutation, crossover and selection.

7.2 TAGUCHI METHOD

Dr. Taguchi of Nippon Telephones and Telegraph Company, Japan has developed a method based on **ORTHOGONAL ARRAY** experiments which gives much reduced variance for the experiment with optimum settings of control parameters. Thus, the marriage of Design of Experiments with optimization of control parameters to obtain best results is achieved in the Taguchi Method. **Orthogonal Arrays** (OA) provide a set of well balanced (minimum) experiments and Dr. Taguchi's Signal-to-Noise ratios (S/N), which are log functions of desired output, serve as objective functions for optimization, help in data analysis and prediction of optimum results. Taguchi method is a scientifically disciplined mechanism for evaluating and implementing improvements in products, processes, materials, equipment, and facilities. These improvements are aimed at improving the desired characteristics and simultaneously reducing the number of defects by studying the key variables controlling the process and optimizing the procedures or design to yield the best results. The method is applicable over a wide range of engineering fields that include processes that manufacture raw materials, sub systems, products for professional and consumer markets. In fact, the method can be applied to any process be it engineering fabrication, computer-aided-design, banking and service sectors etc. Taguchi method is useful for 'tuning' a given process for 'best' results.

Taguchi proposed a standard 8-step procedure for applying his method for optimizing any process

1. Identify the main function, side effects, and failure mode
2. Identify the noise factors, testing conditions, and quality characteristics
3. Identify the objective function to be optimized
4. Identify the control factors and their levels
5. Select the orthogonal array matrix experiment
6. Conduct the matrix experiment
7. Analyze the data, predict the optimum levels and performance
8. Perform the verification experiment and plan the future action.

CHAPTER 8

REFERENCES

1. Yonghong Zhong, Haisheng Fang, Qianli Ma and Xuran Dong, "Analysis of droplet stability after ejection from an inkjet nozzle", Cambridge University , Journal of Fluid Mechanics (2018), vol. 845, pp. 378-391.
2. J.R. Castrej´on-Pita, W.R.S. Baxter, J. Morgan, S. Temple4, G.D. Martin, and I.M. Hutchings, "Future, Opportunities and Challenges of Inkjet Technologies", Published in Atomization and Sprays (2013).
3. Andr´e D. Taylor , Edward Y. Kim, Virgil P. Humes, Jeremy Kizuka, Levi T. Thompson, "Inkjet printing of carbon supported platinum 3-D catalyst layers for use in fuel cells", Journal of Power Sources 171 (2007) 101–106.
4. Bing He, Sucui Yang, Zhangrong Qin, Binghai Wen , Chaoying Zhang, "The roles of wettability and surface tension in droplet formation during inkjet printing", Scientific Reports.
5. J.-T. Yeh, "A VOF-FEM Coupled Inkjet Simulation," Proc. ASME FEDSM'01, New Orleans, Louisiana, 2001.
6. Ayoung Lee, Kai Sudau, Kyung Hyun Ahn, Seung Jong Lee, Norbert Willenbacher, "Optimization of Experimental Parameters to Suppress Nozzle Clogging in Inkjet Printing", American Chemical Society (2012).
7. Mary A. Sukeshini, Ryan Cummins, Thomas L. Reitz, Ryan M. Miller, "Ink-Jet Printing: A Versatile Method for Multilayer Solid Oxide Fuel Cells Fabrication", Journal of the American Ceramic Society, 33rd International conference and exposition on advanced ceramics and composites: 6th International symposium on solid oxide fuel cell.
8. Gwon Deok Han, Kiho Bae, Eun Heui Kang, Hyung Jong Choi, Joon Hyung Shim, "Inkjet Printing for Manufacturing Solid Oxide Fuel Cells", American Chemical Society Energy Letters 2020, 5, 1586−1592.

9. Daehwan Jang, Dongjo Kim, Jooho Moon, "Influence of Fluid Physical Properties on Ink-Jet Printability", American Chemical Society, Langmuir 2009, 25, 2629-2635.
10. Silas Towne, Vish Viswanathan, James Holbery, Peter Rieke, "Fabrication of polymer electrolyte membrane fuel cell MEAs utilizing inkjet print technology", Journal of Power Sources 171 (2007) 575–584.
11. Jiun-Der Yu, Shinri Sakai, J.A. Sethian, "A Coupled Level Set Projection Method Applied to Ink Jet Simulation ", Applied Mathematical Sciences subprogram of the Office of Energy Research, U.S. Department of Energy.
12. Amit Kumar ball, Raju das, Shibendu Shekhar Roy, Dakshina Ranjan Kisku and Naresh Chandra Murmu, "Experimentation modelling and optimization of electrohydrodynamic inkjet microfabrication approach: a Taguchi regression analysis", Indian Academy of Sciences(2019).
13. E. Olsson and G. Kreiss, "A Conservative Level Set Method for Two Phase Flow," J.Comput. Phys., vol. 210, pp. 225–246, 2005.
14. P. Yue, J. Feng, C. Liu, and J. Shen, "A Diffuse-Interface Method for Simulating Two-Phase Flows of Complex Fluids," J. Fluid Mech., vol. 515, pp. 293–317, 2004.
15. Seung-Hwan Kang, San Kim, Dong Kee Sohn, Han Seo Ko, "Analysis of drop-on-demand piezo inkjet performance", Physics of Fluids 32, 022007 (2020).
16. Tim Tofan, Harald Kruggel-Emden, Vytautas Turla and Raimondas Jaseviˇcius, "Numerical Modeling of the Motion and Interaction of a Droplet of an Inkjet Printing Process with a Flat Surface", MDPI Applied Science (2021) 11, 527.
17. A.B. AQEEL, M. MOHASAN, Pengyu LV, Yantao YANG, Huiling DUAN, "Effects of nozzle and fluid properties on the drop formation dynamics in a drop-on-demand inkjet printing", Applied Mathematics and

Mechanics (English Edition), National Natural Science Foundation of China (No. 11802004).

18. Ralph JM, Schoeler AC, Krumpelt, M. Materials for lower temperature solid oxide fuel cells. J Mater Sci2001; 36:1161e72.
19. BOS, A. V. D., MEULEN, M. J. V. D., DRIESSEN, T., BERG, M. V. D., REINTEN, H., WIJSHOFF, H., VERSLUIS, M., and LOHSE, D. Velocity profile inside piezo-acoustic inkjet droplets in flight: comparison between experiment and numerical simulation. Physical Review Applied, 1(1), 014004-1 (2014).
20. Chao Li a, Huangang Shi a, Ran Ran a, Chao Su a, Zongping Shao, “Thermal inkjet printing of thin-film electrolytes and buffering layers for solid oxide fuel cells with improved performance”, international journal of hydrogen energy 38 (2013) 9310e9319.